Nano Research

Open Access

Research Article

Gold nanoparticles promote pathogenic *Salmonella* infection in mice by catalase-mimetic H_2O_2 scavenging

Xinyu Guo[1,§], Mingkai Bai[2,§], Yan Liu[1], Xiumei Jiang[3], Jun-Jie Yin[3], Haohao Wu[2], and Suqin Zhu[1]✉

[1] *Institute of Nutrition and Health, School of Public Health, Qingdao University, Qingdao 266000, China*
[2] *State Key Laboratory of Marine Food Processing & Safety Control, College of Food Science and Engineering, Ocean University of China, Qingdao 266000, China*
[3] *Division of Analytical Chemistry, Office of Regulatory Science, Center for Food Safety and Applied Nutrition, U.S. Food and Drug Administration, College Park, MD 20740, USA*
§ *Xinyu Guo and Mingkai Bai contributed equally to this work.*

Cite this article: *Nano Research*, **2025**, *18*, 94907985. https://doi.org/10.26599/NR.2025.94907985

ABSTRACT: Endogenous H_2O_2 production by intestinal cells and commensal lactic acid bacteria plays an important role in reducing pathogenic infection. Few reports have addressed the influence of catalase-mimetic gold nanoparticles (AuNPs) on intestinal barrier function against invading pathogens. In this study, citrate- and tannic acid-stabilized 5 nm-sized AuNPs were orally administered to C57BL/6 mice daily for 21 day before and during 6 day of *Salmonella enterica* serovar Typhimurium (*S.* Typhimurium) exposure. High-throughput sequencing of fecal 16S rRNA revealed that AuNPs did not significantly alter gut microbiota diversity and community before *S.* Typhimurium challenge. Fecal bacterial enumeration with selective media during the 6-day *S.* Typhimurium challenge period unveiled that AuNPs markedly induced the increased *Salmonella* colonization and the decreased *Lactobacillus* abundance. AuNPs exacerbated *S.* Typhimurium-induced food intake reduction, body weight loss, cecum/colon histopathological lesions, and mortality. *In vitro* growth kinetic and virulence assays demonstrated that AuNPs notably counteracted the H_2O_2-induced suppression of *S.* Typhimurium growth in liquid medium, migration on agar plate, and adhesion and invasion of Caco-2 cell monolayers. In comparison with AuNPs coated by tannic acid, citrate-coated AuNPs exerted significantly greater effects on *S.* Typhimurium-induced weight loss and mortality *in vivo*, as well as *S.* Typhimurium growth, migration, and invasion in the presence of H_2O_2 *in vitro*, which correlated well with the superior catalase-mimetic activity of citrate-coated AuNPs than tannic acid-coated ones in serum-supplemented cell culture media according to the results of electron spin resonance oximetry. Overall, AuNPs may increase the risk of pathogenic *Salmonella* infection through catalytic decomposition of endogenous H_2O_2.

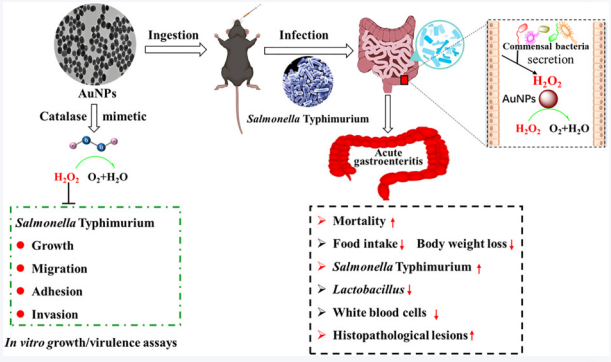

KEYWORDS: gold nanoparticles (AuNPs), *Salmonella enterica* serover Typhimurium (*S.* Typhimurium), intestinal colonization, hydrogen peroxide (H_2O_2), catalase activity

1 Introduction

Nanoparticles are widely applied in diverse areas, yet their unique properties might affect human health [1]. Prospective studies have shown that nanoparticles can reach the intestine, interact with the gut microbiome, and alter the gut microbiota composition [2]. Clinical trial data have confirmed that orally administered gold nanoparticles (AuNPs) at micro-doses as low as 0.34 mg/day exhibit both therapeutic efficacy and safety in patients with rheumatoid arthritis and osteoarthritis [3]. Recently, studies on the effects of nanoparticles (e.g., silver, titanium dioxide, silica dioxide, zinc oxide, and carbon) on gut microbiota have been conducted *in vivo* [3, 4]. However, there are scarce reports of AuNPs on gut microbial profiles. Our previous findings demonstrated that AuNPs reduced the Firmicutes/Bacteroidetes ratio and the abundance of probiotic *Lactobacillus* in mice treated with dextran sulphate sodium (DSS) [5]. Nevertheless, the underlying mechanism remains unclear. The intestinal microbiome is associated with the

Received: June 30, 2025; **Revised:** August 22, 2025
Accepted: August 23, 2025

✉Address correspondence to zhusuqin@qdu.edu.cn

development of diseases such as inflammatory bowel disease, cardiovascular disease, obesity, metabolic syndrome [6]. Therefore, further studies are needed to elucidate the mechanism by which AuNPs alter gut microflora and their potential adverse health effects.

The pathogen *Salmonella enterica* serovar Typhimurium (hereafter referred to as *S.* Typhimurium (*S.* T)) is a leading cause of human gastroenteritis worldwide and serves as a mouse model for human typhoid-like disease [7]. *Salmonella* primarily contaminates milk, meat, poultry, eggs, fruits, and vegetables, and their pathogenic infection can cause diarrhea, fever, and emesis by colonizing the intestine and triggering gut inflammation [8]. The intestinal colonization of food-borne pathogens is hindered by commensal bacteria (e.g., Bacteroides and Firmicutes) through nutrient competition and bacteriostatic substances [9]. *Salmonella* exploits host inflammation to depress commensal microbiota, leveraging gut dysbiosis to facilitate their intestinal colonization [7–9].

Hydrogen peroxide (H_2O_2) plays an essential role as a signaling molecule in host immune responses, and is an integral part of host colonization resistance by suppressing inflammatory responses, enhancing intestinal barrier function, and accelerating tissue restitution [10]. Additionally, H_2O_2 at the luminal surface can drive out bacteria from the epithelial surface, thereby blocking cellular infection [10, 11]. Multiple studies have confirmed that probiotic bacteria defend against potentially pathogenic bacteria in the intestinal tract by secreting bacteriostatic substances such as antibiotics, bacteriocins, and H_2O_2 [12, 13]. AuNPs can eliminate H_2O_2, which significantly weakens the inhibitory effect of lactic acid bacteria on foodborne pathogens (*Escherichia coli*, *Listeria monocytogenes*, and *Staphylococcus aureus*) [5, 14]. Thus, we hypothesize that AuNPs intake might increase the risk of host infection by enhancing *S.* T colonization in the intestinal tract.

In order to validate our speculation, the effects of AuNPs on gut microbiota, *Salmonella* colonization, inflammatory responses, and intestinal barrier function were conducted in a mouse model. The effects of AuNPs on *S.* T growth in liquid medium, migration on agar plate, and adhesion and invasion of Caco-2 cell monolayers in the absence or presence of H_2O_2 were evaluated *in vitro*.

2 Materials and methods

2.1 Reagents

4-Hydroxy-2,2,6,6-tetramethylpiperidine-1-^{15}N-oxyl (^{15}N-PDT) was supplied by Cambridge Isotope Laboratories, Inc. (Andover, MA, USA). Citrate- and tannic acid-stabilized 5 nm-sized AuNPs (hereafter referred to as Au-5 nm/Citrate and Au-5 nm/TA, respectively) were provided in 0.1 mM phosphate buffered saline (PBS) by CytoDiagnostics (Burlington, Canada). Luria-Bertani (LB) broth, LB agar, deMan, Rogosa and Sharpe (MRS) broth, MRS agar, Bifidum Selective Medium (BSM) Agar, Violet Red Bile Dextrose (VRBD) agar, and Bismuth Sulfite (BS) agar were purchased from Qingdao Hope Biotechnology. The enhanced chemiluminescence (ECL) detection kit, and sandwich enzyme-linked immunosorbent assay (ELISA) kits for mouse interleukin-6 (IL-6), Dulbecco's modified Eagle medium (DMEM), Dulbecco's phosphate-buffered saline (DPBS) and tumor necrosis factor-α (TNF-α) were obtained from Thermo Fisher Scientific (CA, USA). The H_2O_2 quantitative assay kit was provided by Sangon Biotech (Shanghai, China). Rabbit anti-mouse NF-kB p65 polyclonal antibody (ab32536), horseradish peroxidase (HRP)-conjugated goat anti-mouse IgG secondary antibody (ab6789), HRP-conjugated goat anti-rabbit IgG secondary antibody (ab205718), mouse monoclonal anti-β-actin antibody (ab6276), occludin (ab167161), heat-shock protein 25 (Hsp25) and claudin-4 (ab15104) were bought from Abcam (Shanghai, China).

2.2 *Salmonella* strain and culture conditions

S. T CICC 21483 from the China Center of Industrial Culture Collection (Beijing, China) was used to challenge the animals. *S.* T was routinely cultured in LB broth at 37 °C, and viable cells were enumerated on BS agar plates. The overnight-cultured *S.* T cells were harvested by 10-min centrifugation at 8000*g*, and their resuspension in sterile PBS was used to challenge the mice.

2.3 Animal experiments

Male C57BL/6J mice (6–7 weeks old, weighing 20.7 ± 1.1 g) were provided by Lukang Pharmaceutical Co. (Shandong, China). Animals were maintained in individual cages in an air-conditioned room (20–24 °C, 55%–65% humidity) under a lighting regime of 12 h light: 12 h dark, and received *ad libitum* a pelletized chow diet (TROPHIC Animal Feed High-Tech Co., Ltd., Nantong, China) and pure water for the course of the entire experiment. All experiments were performed ethically in accordance with the principles in the National Institutes of Health *Guide for the Care and Use of Laboratory Animals* and were approved by the Committee on the Ethics of Animal Experiments of Ocean University of China.

Following 7 day of acclimation, the mice were randomly assigned to normal control group (n = 8), *S.* T control group (n = 8), Au-5 nm/Citrate+*S.* T group (n = 8), and Au-5 nm/TA+*S.* T group (n = 8). The normal control and *S.* T control groups were intragastrically administered with 200 μL PBS once per day per mouse during the 21-day experimental period, while the AuNPs-treated groups received 200 μL of Au-5 nm/Citrate (2.75 μg/mL) or Au-5 nm/TA (2.75 μg/mL) once per day per mouse during the 21-day experimental period. The oral gavage dosage of AuNPs corresponded to 0.55 μg gold/animal and was approximately equivalent to 25 μg gold/kg body weight. This dosage was previously reported to be effective for AuNPs to protect against colitis [5].

To challenge the mice, *S.* T was administered to the *S.* T control and AuNPs-treated groups by oral gavage at a dose of 2.0×10^8 CFU in 200 μL sterile PBS once per day per mouse since the 16th day [15, 16]. Survival rate, food intake and body weight were daily recorded from the 17th to 22nd day. Blood was collected for hematology measurements before mice were sacrificed on the 22nd day. For hematological analysis, blood samples were immediately collected into tubes containing ethylenediamine tetra-acetic acid and then analyzed on an XN-9000 hematology analyzer (Sysmex, Kobe, Japan). Spleen, liver, cecum, and colon were collected for further tests.

2.4 Gut microbiota analysis

Before the challenge with *S.* T on the 16th day, fecal samples were collected to assay gut microbiota. High-quality DNA was extracted from the samples according to the manufacturer's instructions. The DNA quality and quantity were measured by 1% agarose gel electrophoresis and ultraviolet spectrophotometer, respectively. The primers of 515F (5'-GTGYCAGCMGCCGCGGTAA-3') and 907R

(5'-CCYCAATTCMTTTRAGTTT-3') were used for amplifying the V4-V5 regions of 16S rDNA gene. The 16S rRNA tag-encoded high-throughput sequencing was performed on an Illumina HiSeq 2500 high-throughput sequencer (Illumina, SD, USA) at Shanghai Personalbio Technology Co., Ltd. (Shanghai, China). The data analysis procedure using FLASH, QIIME, and UPARSE pipelines was consistent with our previous report [5].

2.5 Bacterial enumeration

Salmonella, *Lactobacillus*, *Bifidobacterium bifidum*, and *Enterobacteriaceae* in feces collected every two days since the 16th day were enumerated on BS agar, MRS agar, BSM agar, and VRBD agar, respectively. *Salmonella* in liver and spleen were enumerated on BS agar. *Salmonella*, *Lactobacillus*, and *Enterobacteriaceae* were aerobically cultured at 37 °C for 24–48 h before being enumerated. *B. bifidum* were anaerobically cultured at 37 °C for 48 h before being enumerated. In the VRBD agar, the purple colonies were enumerated as the *Enterobacteriaceae* count.

2.6 Biochemical measurements

Pre-weighed proximal colonic segments were homogenized with 25 volumes of radioimmunoprecipitation assay buffer containing phenylmethylsulfonyl fluoride (1 mM) and protease and phosphatase inhibitor cocktails in a homogenizer tube containing ceramic beads using a Bioprep-6 Homogenizer (Aosheng, China). The homogenate was centrifuged at 4 °C (5 min × 10,000*g*), and the supernatant was used as the tissue extract.

The levels of IL-6 and TNF-α in the tissue extracts were assayed using ELISA kits following the manufacturer's instructions. The protein concentration in the tissue extract was determined with the Pierce BCA protein assay kit according to the manufacturer's instructions. Protein in the tissue extract was denatured in SDS-loading buffer, separated with SDS–PAGE gel electrophoresis, and then blotted onto a PVDF membrane. After blocking in Tris buffered saline with Tween 20 (TBST) (10 mM Tris (pH 7.5), 150 mM NaCl, and 0.05% Tween 20) supplemented with 5% fat-free dried milk at room temperature for 1 h. Then the membrane was incubated overnight at 4 °C with anti-β-actin (1:5000 dilution), anti-NF-κB p65 (1:8000 dilution), anti-Claudin-4 (1:200 dilution), anti-Hsp-25 (1:1000 dilution), or anti-Occludin (1:300 dilution). After 1-h incubation at room temperature with HRP-conjugated secondary antibodies (1:6000 dilution), the immune complexes were washed with TBST for three times and visualized with an ECL detection kit on a Tanon-5200 Multi image analyzer (Tanon Science & Technology Co., Ltd., Shanghai, China).

2.7 Histopathological examination

A 1-cm segment of cecum and proximal colon was fixed in 4% paraformaldehyde, desiccated, and embedded in paraffin. The paraffin-embedded colonic tissues were cut into 5-μm thickness slices before routine hematoxylin and eosin (H&E) staining. Histologic observation was performed under a Nikon Eclipse Ti-SR microscope equipped with a Nikon DS-U3 digital camera (Tokyo, Japan). Ten randomly selected fields were imaged for each sample, and the histological lesions in these fields were scored according to previous reports [5]. A mean score of 16 fields was employed as the histologic score for each animal.

2.8 *In vitro* growth and migration assay of *S.* T

S. T were cultured in LB broth with or without containing H_2O_2 (250 μM), AuNPs (0.6 μg/mL), and bovine catalase (10 U/mL) at 37 °C with shaking (160 r/min) and light protection by aluminum foil for 8 h. Viable *Salmonella* counts were enumerated on BS agar. H_2O_2 concentrations were assayed using the H_2O_2 quantification assay kit. The growth kinetics were described using the modified Gompertz model, which uses a static equation to describe bacterial growth as a function of time [17].

$$\lg N(t) = \lg N_0 + \lg\frac{N_{\max}}{N_0} \times \exp\left\{-\exp\left[\frac{\mu_{\max} \times 2.718}{\lg(N_{\max}/N_0)} \times (Lag - t) + 1\right]\right\} \quad (1)$$

where N (CFU/mL) is the population density at time t (h) (the index 0 denotes initial values), μ_{max} is the maximum specific growth rate (lg(CFU/(mL·h))), N_{max} is the final maximum cell population (CFU/mL), *Lag* is the lag time (h) .

The migration of *S.* T was tested on LB agar with or without containing AuNPs (0.6 μg/mL) or bovine catalase (10 U/mL) as described by Botteaux et al. [16]. Briefly, the *S.* T culture (OD = 0.4–0.6) was dropped onto the center of an agar plate, followed by pasting a filter paper disk saturated with H_2O_2 (250 μM) or H_2O on agar plate surfaces, and the plates were incubated at 37 °C with light protection by aluminum foil for 14 h before observing the bacterial zone.

2.9 *In vitro* adhesion and invasion assay of *S.* T

Caco-2 cells were originally obtained from the Cell Bank of the Chinese Academy of Sciences (Shanghai, China) and were routinely cultured in DMEM medium supplemented with 10% fetal bovine serum at 37 °C in a humidified atmosphere containing 5% CO_2. Caco-2 cells seeded in 24-well transwell inserts (0.4 μm pore size, Corning, Shanghai, China) at a density of 2×10^4 cells per well were cultured for > 10 day to form a monolayer with the transepithelial electrical resistance over 1000 Ω·cm^2. *S.* T was cultured in LB broth for 10 h, harvested by centrifugation (8000 r/min × 5 min), washed two times with DPBS, and re-suspended in DMEM medium with or without containing AuNPs (100 ng/mL) and H_2O_2 (250 μM) at a density of 8×10^7 CFU/mL. The medium in the upper transwell chamber was replaced with 200 μL of the bacterial suspension. For the adhesion assay, Caco-2 cells and *S.* T were co-cultured for 1 h, and then Caco-2 cells were washed three times with DPBS before being harvested for bacterial enumeration on BS agar according to Burkholder and Bhunia's method [18]. For the invasion assay, Caco-2 cells and *S.* T were co-cultured for 3 h, and then Caco-2 cells were washed three times with DPBS before being treated with gentamycin (150 μg/mL in DPBS) in the upper chamber for 1 h and harvested for bacterial enumeration on BS agar. The residual H_2O_2 in the upper chamber medium after co-culture was determined using the H_2O_2 quantification assay kit.

2.10 Electron spin resonance (ESR) oximetry assay

ESR oximetry technique was applied to analyze the catalase-mimetic activity of AuNPs. The reaction mixture consisted of H_2O_2 (10 mM), AuNPs (28 μg/mL), and ^{15}N-PDT (0.2 mM) in DMEM supplemented with 10% fetal bovine serum. Data acquisition began 1 min after sample mixing, and the spectra were recorded with a Bruker EMX ESR spectrometer (Billerica, MA, USA) using the following settings: 1 mW microwave power, 0.05 G field modulation, and 2 G scan range. The oxygen production was estimated using the increase in peak-to-peak line width of the ^{15}N-

PDT lower field ESR line as described previously [5].

2.11 Statistical analysis

Statistical analyses were done using SPSS software version 19.0 (SPSS, Inc., Chicago, USA) and OriginPro 7.0 software (OriginLab Co., Northampton, USA). One-way analysis of variance (ANOVA) followed by post-hoc Least Significant Difference (LSD) test or Wilcoxon signed-rank test was used to compare the mean differences. Significant differences were defined at probability values (P-values) of $P < 0.05$.

3 Results and discussion

3.1 AuNPs had no observable toxical effect on healthy mice

Studies have demonstrated that various nanomaterials exhibit no significant toxicity to human cells, zebrafish, mice, or pigs at low doses [19, 20]. Body weight and food intake are basic parameters to assess the potential toxicity of various nanomaterials [21]. In the present study, oral administration of AuNPs at the dose of 25 μg gold/kg/day demonstrated no significant adverse effect on body weight and food intake over the 15-day experimental period before *S.* T exposure (Figs. S1(a) and S1(b) in the Electronic Supplementary Material (ESM)). Gut microbiota constitutes an indispensable part of the intestinal barrier against invading pathogens. To investigate whether AuNPs could induce gut dysbiosis in healthy mice, fecal samples at the 16th day before *S.* T exposure were collected for high-throughput sequencing analysis of gut microbiota diversity. The rarefaction curves (Fig. S2 in the ESM) reached a plateau, indicating sufficient recovery of bacterial taxa in the fecal samples. The treatments with AuNPs induced no significant difference in α-diversity (i.e., phylotype richness) as measured by the indices of Shannon and Simpson (Fig. 1(a)). Principal coordinate analysis (PCoA) was performed to evaluate the β-diversity (i.e., between-sample diversity) based upon weighted unique fraction distances (Fig. 1(b)). The three groups did not cluster separately, suggesting that AuNPs did not significantly affect the community structure of gut microbiota in healthy mice. The comparison of microbial communities at the genus level was visualized by heat-map (Fig. 1(c)). The relative abundances of the top 20 genus showed no significant difference among the three groups. Collectively, our findings demonstrate that the 15-day oral administration of AuNPs to healthy C57BL/6J mice at the tested dose did not induce significant alterations in body weight, food consumption, and gut microbiota diversity and community. These observations were in consistent with the findings of Wang et al. (2019) that the 3-day oral exposure to gold nanoclusters did not significantly change the gut microbiota diversity and community in healthy BALB/c mice [22]. However, AuNPs seem to alter gut microbial diversity and structure in disease-modeled animals such as osteoarthritis and ulcerative colitis mice [5, 23].

3.2 AuNPs exacerbated *Salmonella* infection in mice

The *S.* T control animals suffered from significant loss of appetite and body weight compared to the normal controls after *S.* T challenge for 6 days according to the results of food intake and body weight ($P < 0.05$) (Figs. 2(a) and 2(b)). AuNPs significantly aggravated these *S.* T-associated symptoms ($P < 0.05$). Citrate-coated AuNPs displayed a more prominent effect on weight loss

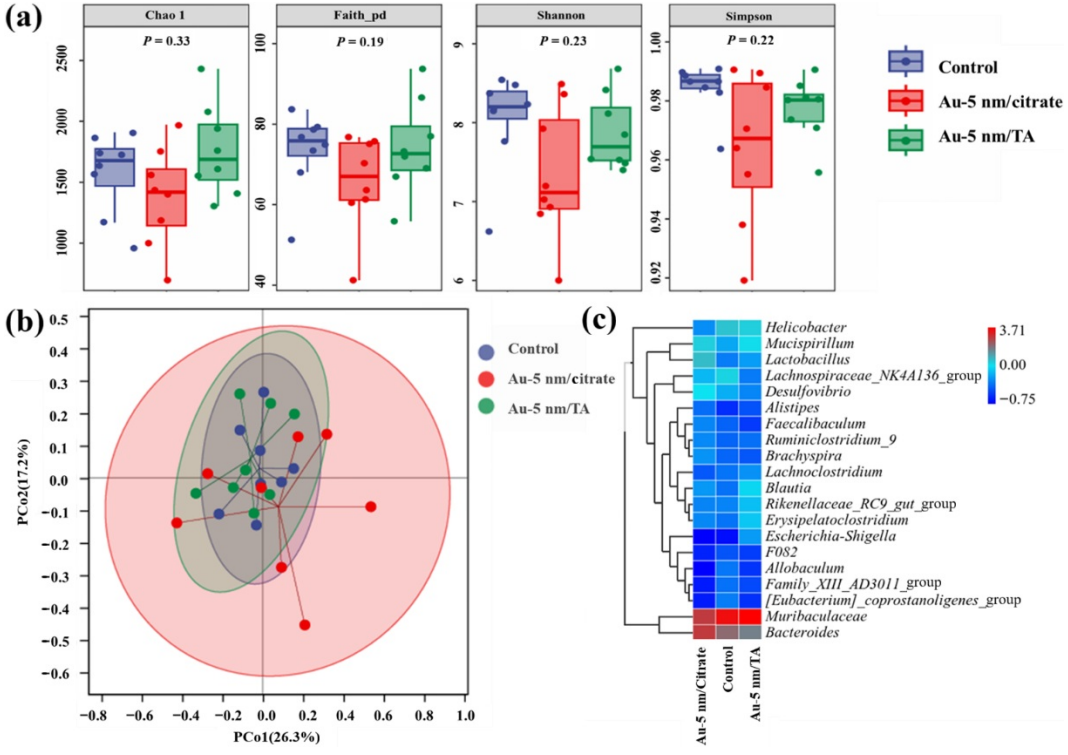

Figure 1 The diversity of gut microbiota in healthy mice with or without being orally administered with AuNPs for 15 days: (a) the box plot of alpha diversity using the Chao1, Faith, Shannon, and Simpson metrics; (b) a principal coordinate (PCoA) plot of weighted unique fraction distances, where each point represents a single sample. The percentages indicate the contribution of principal components to the difference of samples; (c) a heat-map comparison of the relative abundances of the top 20 genus in microbial communities.

than tannic acid-coated ones ($P < 0.05$). Figure 2(c) displays the post-infection survival curves for all the groups, and after *S.* T challenge for 4 days, the survival rates were at 100%, 87.5%, 75%, and 62.5% for the groups of normal control, *S.* T control, Au-5 nm/TA+*S.* T, and Au-5 nm/citrate+*S.* T, respectively. There was 1 death in the *S.* T control group on the 4th day post-infection. Two deaths appeared in the Au-5 nm/TA+*S.* T group on the 2nd and 4th day post-infection. The Au-5 nm/citrate+*S.* T group had 3 deaths on the 2nd, 3rd, and 4th day post-infection. Apparently, AuNPs increased the *S.* T-induced mortality, and such effect was more prominent for citrate-coated AuNPs than tannic acid-coated ones. Our observations were inconsistent with the findings of Li et al. (2019) that AuNPs cure bacterial infection in Balb/c mice by benefiting intestinal microflora [24]. This might be explained by the usage of AuNPs coated by 4,6-diamino-2-pyrimidinethiol, a compound inhibits *Escherichia coli* itself, in the study of Li et al. (2019). In fact, AuNPs need to be functionalized with antibacterial compounds to serve as bactericidal agents against multi-drug-resistant bacteria [25].

3.3 AuNP increased intestinal *Salmonella* colonization and histological lesions in mice

Figure 3(a) shows the fecal shedding of viable *Salmonella* cells by mice during the *S.* T challenge period. There were remarkably greater levels of fecal *Salmonella* in the *S.* T control group than the normal control group ($P < 0.05$), confirming the good intestinal colonizing capacity of *S.* T. The AuNPs-treated groups had significantly more abundant fecal viable *Salmonella* cells than the *S.* T control group from the 4th day post-infection ($P < 0.05$), suggesting the increased intestinal colonization of *S.* T by orally administered AuNPs. According to the viable cell counts of *Lactobacillus*, *B. bifidum*, and *Enterobacteriaceae* in feces (Figs. 3(b)–3(d)), *S.* T infection resulted in the reduced *Lactobacillus* abundance and the increased *Enterobacteriaceae* abundance in gut microbiome ($P < 0.05$). These observations were consistent with the findings of Stecher et al. (2007) that *Salmonella* infection caused a reduction in the intestinal abundance of beneficial *Lactobacillus* in mice [9]. AuNPs significantly aggravated the *S.* T-induced reduction in intestinal *Lactobacillus* abundance ($P < 0.05$), but exerted no significant effect on the intestinal abundances of *B. bifidum*, and *Enterobacteriaceae* ($P > 0.05$).

Extensive research has established that *Lactobacillus* exerts antimicrobial effects against multiple invading pathogens, including *S.* T SL1344, *Gardnerella vaginalis* DSM 4944, and *Escherichia coli* CFT073 through the secretion of bactericidal metabolites such as H_2O_2 and bacteriocins [26, 27]. Our previous study demonstrated that AuNPs inhibit the antagonistic action of *Lactobacillus gasseri* toward foodborne enteric pathogens (i.e., *S.* T, *E.* coli, *Listeria monocytogenes*, and *Staphylococcus aureus*) in associative cultures through their H_2O_2-scavenging action [14]. We thus hypothesize that AuNPs may promote intestinal *S.* T colonization by counteracting the H_2O_2-mediated antimicrobial defense of *Lactobacillus* in the gut microenvironment. Bifidobacterium abundance was unaffected by AuNPs likely because its growth inhibition mechanisms against *Salmonella* (e.g., producing bacteriocins) are H_2O_2-independent and thus not disrupted by

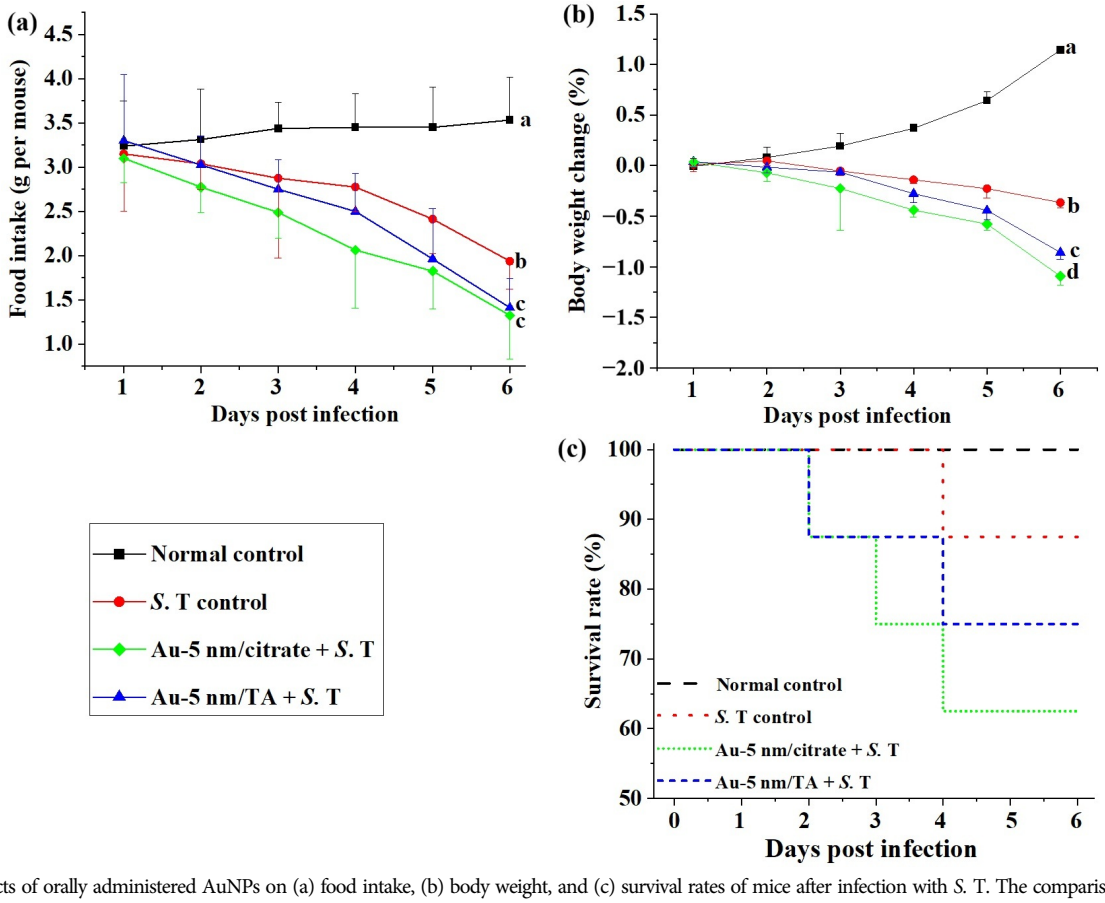

Figure 2 Effects of orally administered AuNPs on (a) food intake, (b) body weight, and (c) survival rates of mice after infection with *S.* T. The comparison is made by using one-way ANOVA with LSD, and different lower-case letters marking significant differences ($P < 0.05$).

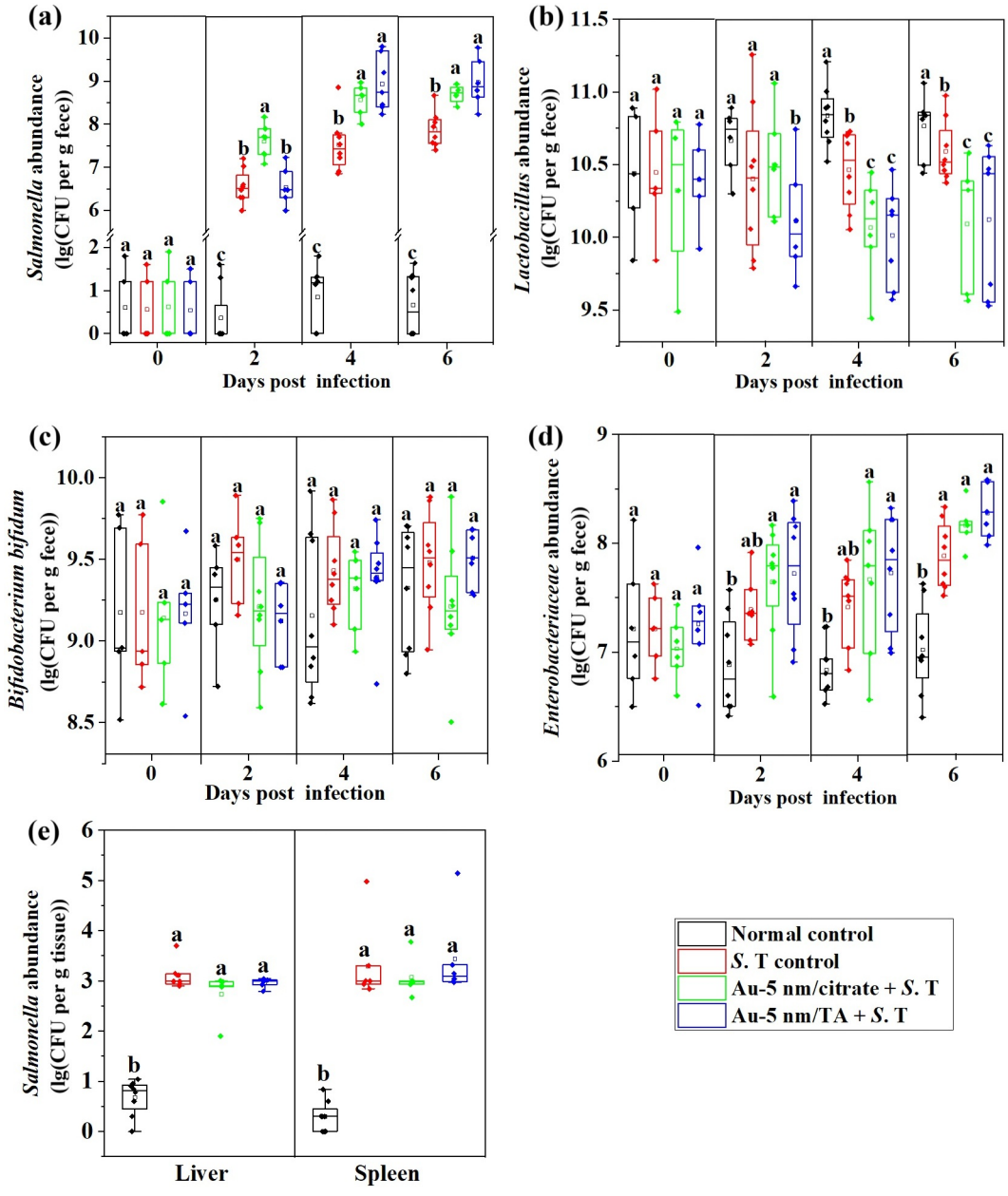

Figure 3 Effects of orally administered AuNPs on the fecal shedding of viable (a) *Salmonella*, (b) *Lactobacillus*, (c) *Bifidobacterium bifidum*, and (d) *Enterobacteriaceae*, as well as (e) the liver and spleen *Salmonella* abundances, in mice after infection with *S.* T. The comparison is made by using one-way ANOVA with LSD, and different lower-case letters marking significant differences ($P < 0.05$).

AuNP-mediated H_2O_2 scavenging. Enterobacteriaceae abundance remained unchanged possibly because Salmonella-induced inflammation already elevated this group, and AuNPs primarily exacerbated Salmonella colonization through H_2O_2 decomposition without further altering Enterobacteriaceae proliferation beyond the infection-induced baseline.

Previous studies have demonstrated that *S.* T infection induces acute colitis in murine models [9, 15, 28]. Histopathological examination of cecal and colonic tissues (Figs. 4(a) and 4(b)) demonstrated prominent edema of muscularis mucosa as evidenced by ~ 2-fold thickened mucin layer and evident inflammatory cell infiltration within both the mucosal and submucosal layers in the *S.* T control mice, confirming the occurrence of acute colitis associated with *Salmonella* infection. These histopathological manifestations were more intense in AuNPs-treated groups than in *S.* T control group. By using histological scoring, we found that AuNPs significantly aggravated the *S.* T-associated histological lesions ($P < 0.05$) (Figs. 4(c) and 4(d)), which was in line with their effect on increasing intestinal *Salmonella* colonization (Fig. 3(a)).

3.4 AuNPs did not aggravate *Salmonella* translocation and inflammatory responses in mice

To monitor *S.* T translocation from the gut, viable *Salmonella* cells in spleen and liver were enumerated at the end of the challenge period. As shown in Fig. 3(e), there were remarkably higher levels of *Salmonella* abundance in liver and spleen of the S. T control group compared to the normal control group, confirming

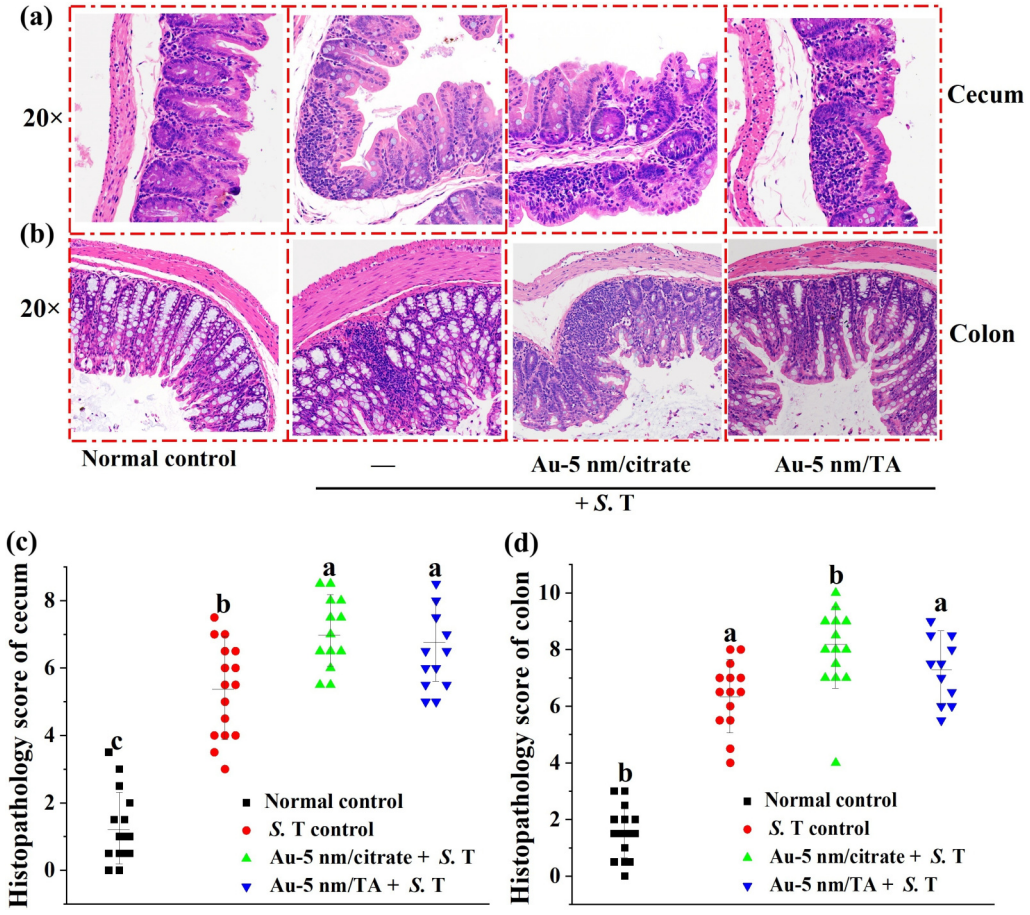

Figure 4 Histopathological examination of hematoxylin & eosin-stained intestinal sections from mice infected with *S.* T: the typical images of (a) cecum and (b) colon, and the histological scores of (c) cecum and (d) colon. The comparison is made by using one-way ANOVA with LSD with different lower-case letters marking significant differences ($P < 0.05$).

Salmonella translocation from the gut in *S.* T-infected mice. The AuNPs-treated groups showed liver and spleen *Salmonella* abundances not significantly higher than those of the *S.* T control group ($P > 0.05$), implying that AuNPs did not aggravate *Salmonella* translocation.

Salmonella infection is known to initiate host inflammatory responses via stimulating the production of pro-inflammatory cytokines such as TNF-α and IL-6 by different types of cells, including epithelial cells, macrophages, dendritic cells, and neutrophils [9, 15, 28]. The AuNPs-treated groups had significantly lower levels of peripheral white blood cells than the *S.* T control group ($P < 0.05$) (Fig. 5(a)) and showed peripheral and colonic levels of IL-6 and TNF-α not significantly higher than those of the *S.* T control group ($P > 0.05$) (Figs. 5(b)–5(d)). Based on these observations, AuNPs did not aggravate *S.* T-induced inflammatory responses, and even appeared to reduce systematic inflammation according to the results of white blood cells. AuNPs have been widely studied in biomedicine for their anti-inflammatory effects and their potential for treating neurological and autoimmune disorders [29]. Our previous study has demonstrated that AuNPs could abate intestinal inflammation induced by dextran sodium sulfate (DSS) [5]. In this study, despite their effects on increasing intestinal *Salmonella* colonization and intestinal histological lesions (Figs. 3 and 4), AuNPs did not exacerbate systematic and colonic inflammation most probably due to their anti-inflammatory activity. This independent immune suppression may blunt the host's pro-inflammatory cytokine production despite more severe intestinal tissue damage from increased *Salmonella* colonization, while also not promoting bacterial translocation as the suppressed immune response does not enhance pathogen spread to extraintestinal organs like the liver and spleen.

3.5 AuNPs counteracted the inhibitory effects of H_2O_2 on *S.* T growth, migration, adhesion and invasion *in vitro*

To gain insight into the underlying mechanism of AuNPs' enhancement of *S.* T infection, we systematically evaluated the *in vitro* effects of H_2O_2 on *S.* T growth kinetic and virulence traits in the absence or presence of AuNPs. As shown in Table 1, H_2O_2 (250 μM) significantly resulted in the prolonged lag phase and the decreased maximum growth rate of *S.* T ($P < 0.05$), but had no effect on the maximum cell density of *S.* T ($P > 0.05$). Apparently, H_2O_2 could retard the growth of *S.* T. AuNPs and bovine catalase remarkably counteracted these effects of H_2O_2 on *S.* T growth with citrate-coated AuNPs showing a significantly greater antagonizing effect on maximum growth rate than tannic acid-coated ones ($P < 0.05$) (Table 1). These results demonstrate that AuNPs can protect *S.* T from H_2O_2 stress. Pridmore et al. (2008) reported that H_2O_2 produced by *L. gasseri* effectively killed *S.* T SL1344 [26]. Our previous study also found that AuNPs reduced H_2O_2 accumulation by > 50% in *L. gasseri* culture, thereby significantly attenuating the growth-inhibitory effect of *L. gasseri* on *S.* T in co-culture systems [14].

H_2O_2 is a bacterial repellent that inhibits *Salmonella* migration as

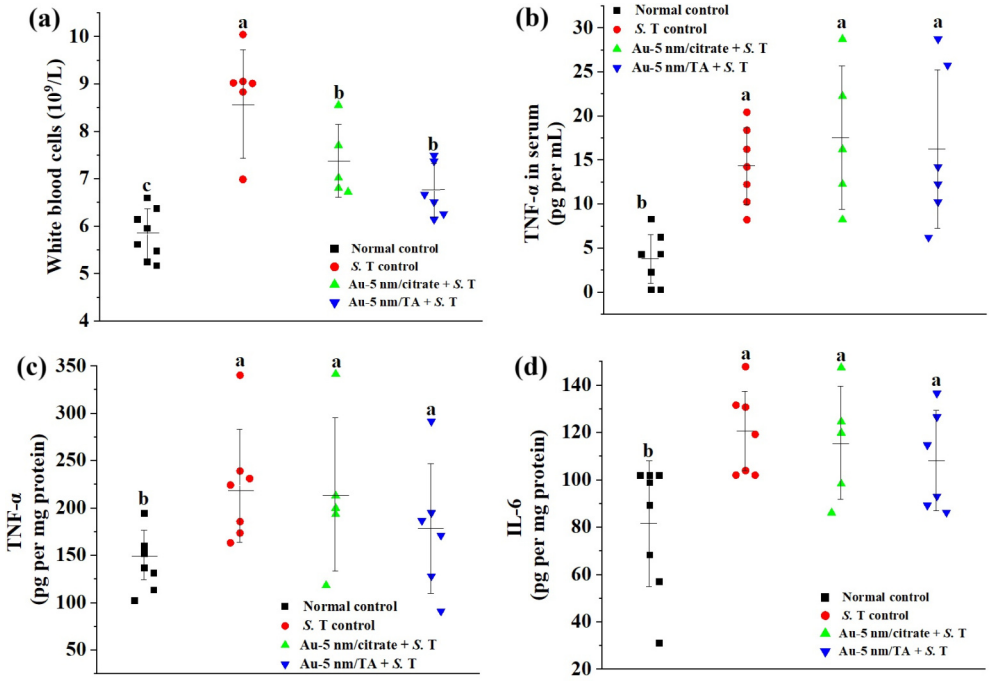

Figure 5 Effects of orally administered AuNPs on the peripheral levels of (a) white blood cells and (b) TNF-α and the colonic levels of (c) TNF-α and (d) IL-6 in mice after infection with *S.* T. The comparison is made by using one-way ANOVA with LSD with different lower-case letters marking significant differences ($P < 0.05$).

Table 1 Effects of AuNPs on the growth kinetics of *S.* T in the presence of 200 μM H_2O_2

	Lag (h)	μ_{max} (h)	lg(N_{max} (CFU/mL))	R^2
Control	2.284 ± 0.038^a	0.708 ± 0.004^e	8.67 ± 0.12	0.996
H_2O_2 + water	2.502 ± 0.033^b	0.603 ± 0.008^f	8.66 ± 0.04	0.997
H_2O_2 + catalase	2.278 ± 0.031^c	0.699 ± 0.005^e	8.64 ± 0.06	0.996
H_2O_2 + Au-5nm/citrate	2.384 ± 0.015^d	0.679 ± 0.004^g	8.73 ± 0.08	0.999
H_2O_2 + Au-5nm/TA	2.386 ± 0.017^d	0.654 ± 0.003^h	8.69 ± 0.03	0.999

$^{a–h}$Data are expressed as the mean ± standard deviations ($n = 3$). Different superscript letters (a–d) denote statistically significant differences of *Lag* (h) ($P < 0.05$); different superscript letters (e–h) denote statistically significant differences of μ_{max} (h) ($P < 0.05$).

reported by Botteaux et al. [30]. In the present study, H_2O_2 significantly inhibited the migration of *S.* T on agar plates, and this effect was remarkably antagonized by AuNPs and bovine catalase with citrate-coated AuNPs showing a significantly greater antagonizing effect than tannic acid-coated ones ($P < 0.05$) (Fig. 6). Previous studies have reported that AuNPs were non-toxic to *S.* T TA102 and could penetrate bacterial cells [31]. Our earlier work also confirmed that AuNPs had no significant effect on *S.* T growth [14]. We therefore conclude that AuNPs counteract the inhibitory effect of H_2O_2 on *S.* T migration by catalytic decomposition of H_2O_2.

As shown in Figs. 7(a) and 7(c), H_2O_2 treatment reduced the adhesion and invasion capabilities of *S.* T against Caco-2 cell monolayers by 21.2% and 87.9%, respectively. The presence of AuNPs completely antagonized the inhibitory effect of H_2O_2 on *S.* T adhesion. The H_2O_2-induced loss of *S.* T invasion capacity partially recovered by 27.5% and 11.3% in the presence of AuNPs coated by citrate and tannic acid, respectively. According to the residual levels of H_2O_2 in the co-culture medium (Figs. 7(b) and 7(d)), citrate-coated AuNPs were more efficient in catalyzing H_2O_2 decomposition than tannic acid-coated ones. This correlated well with their catalase-mimetic activities in serum-supplemented DMEM as determined by ESR oximetry (Fig. 7(e)).

H_2O_2 can prevent hosts from bacterial infection by repelling pathogen colonization, with its production being one key mechanism through which lactic acid bacteria antagonize pathogenic microorganisms [11, 12]. In the present study, AuNPs mitigated the inhibitory effects of H_2O_2 on *S.* T growth, migration, adhesion, and invasion by catalase-mimetic scavenging of H_2O_2 (Figs. 6 and 7). These observations align with the findings in multiple previously published reports [14, 23, 30, 32], suggesting that H_2O_2 scavenging likely represents the primary mechanism of AuNPs to enhance *S.* T infection.

AuNPs may also alter the gut microenvironment through additional mechanisms beyond H_2O_2 scavenging. AuNPs reduced systemic inflammation (Fig. 5(a)) by suppressing white blood cell counts, potentially compromising immune clearance of pathogens and creating a permissive environment for *Salmonella* expansion. AuNPs may directly disrupt protective bacteria (e.g., *Lactobacillus*) via physical interactions or metabolic interference, as evidenced by their aggravated reduction (Fig. 3(b)), independent of H_2O_2 scavenging. Nanoparticle-bacterial complexes could physically facilitate *Salmonella* adhesion to epithelial cells, though this requires experimental validation beyond the current study. These mechanisms likely synergize with catalase-mimetic activity to destabilize colonization resistance.

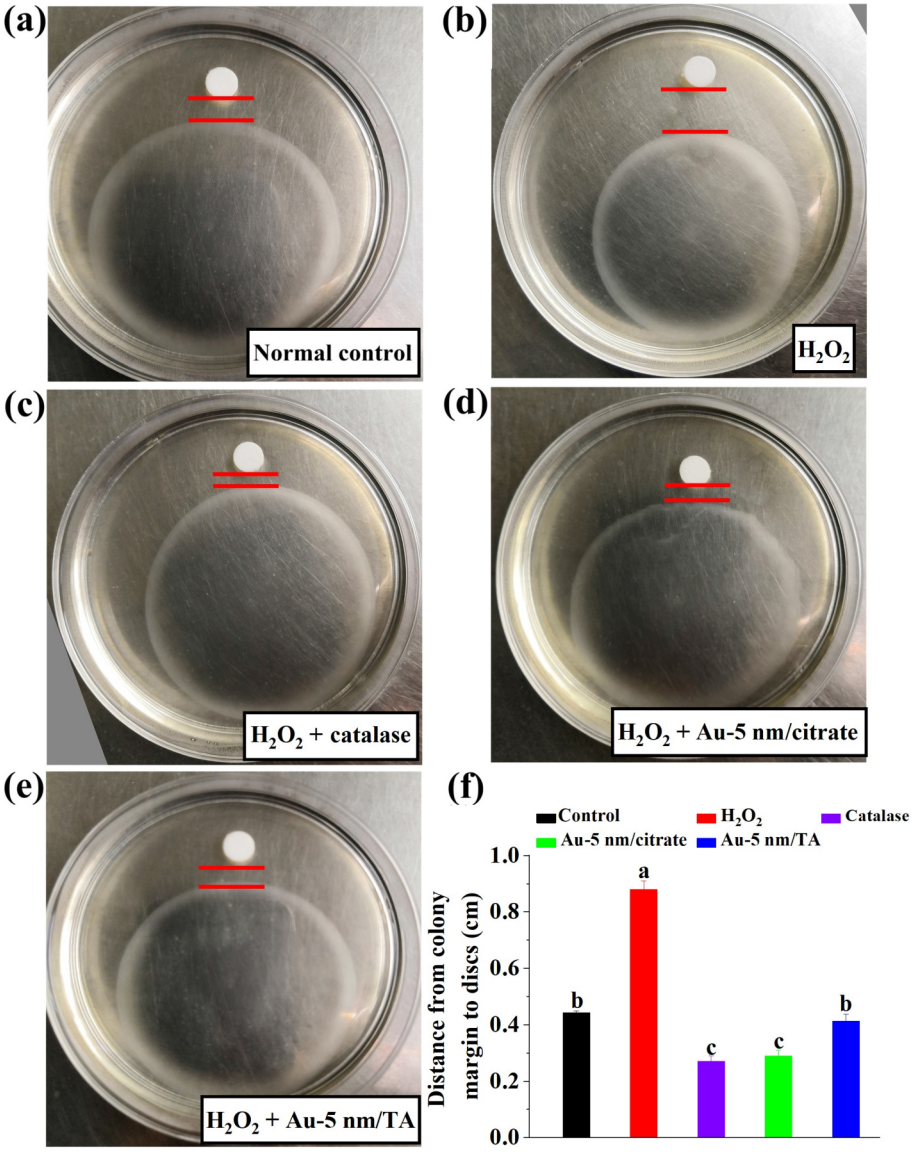

Figure 6 Effects of AuNPs on *S.* T migration in the presence of H_2O_2: (a)–(e) the typical images of bacterial zones and (f) the measurements of distances from filter paper to bacterial zone. The comparison is made by using one-way ANOVA with LSD with different lower-case letters marking significant differences ($P < 0.05$).

4 Conclusion

Despite that orally administered AuNPs had no observable effect on gut microbiota, food intake, and body weight in healthy mice, they aggravated *S.* T-associated apatite reduction, weight loss, histopathological lesions, and mortality mainly through increasing intestinal *Salmonella* colonization, rather than exacerbating pathogen translocation and inflammatory responses. Specifically, AuNPs counteracted the inhibitory effects of H_2O_2 on *S.* T growth, migration, adhesion and invasion *in vitro* through catalase-mimetic H_2O_2 scavenging, thereby providing a possible explanation for their promotion of *S.* T infection *in vivo*. Overall, AuNPs may increase the risk of pathogenic *Salmonella* infection through catalytic decomposition of endogenous H_2O_2.

Electronic Supplementary Material: Supplementary material (Fig. S1 effects of orally administered AuNPs on the kinetics of food intake and body weight in mice before the challenge with *S.* T; Fig. S2 rarefaction curves calculated for each fecal sample) is available in the online version of this article at https://doi.org/10.26599/NR.2025.94907985.

Data availability

All data needed to support the conclusions in the paper are presented in the manuscript and the ESM. Additional data related to this paper may be requested from the corresponding author upon request.

Acknowledgements

This study was financially supported by National Natural Science Foundation of China (No. 82003444), Hainan Province's Key Research and Development Project (No. ZDYF2024XDNY191), Major Science and Technology Project of Haikou City (No. 2023-001), Science and Technology Innovation Program of Sanya City (No. 2022KJCX59), Yantai Development Zone Science and Technology Leading Talent Project (No. 2021RC014), and Major

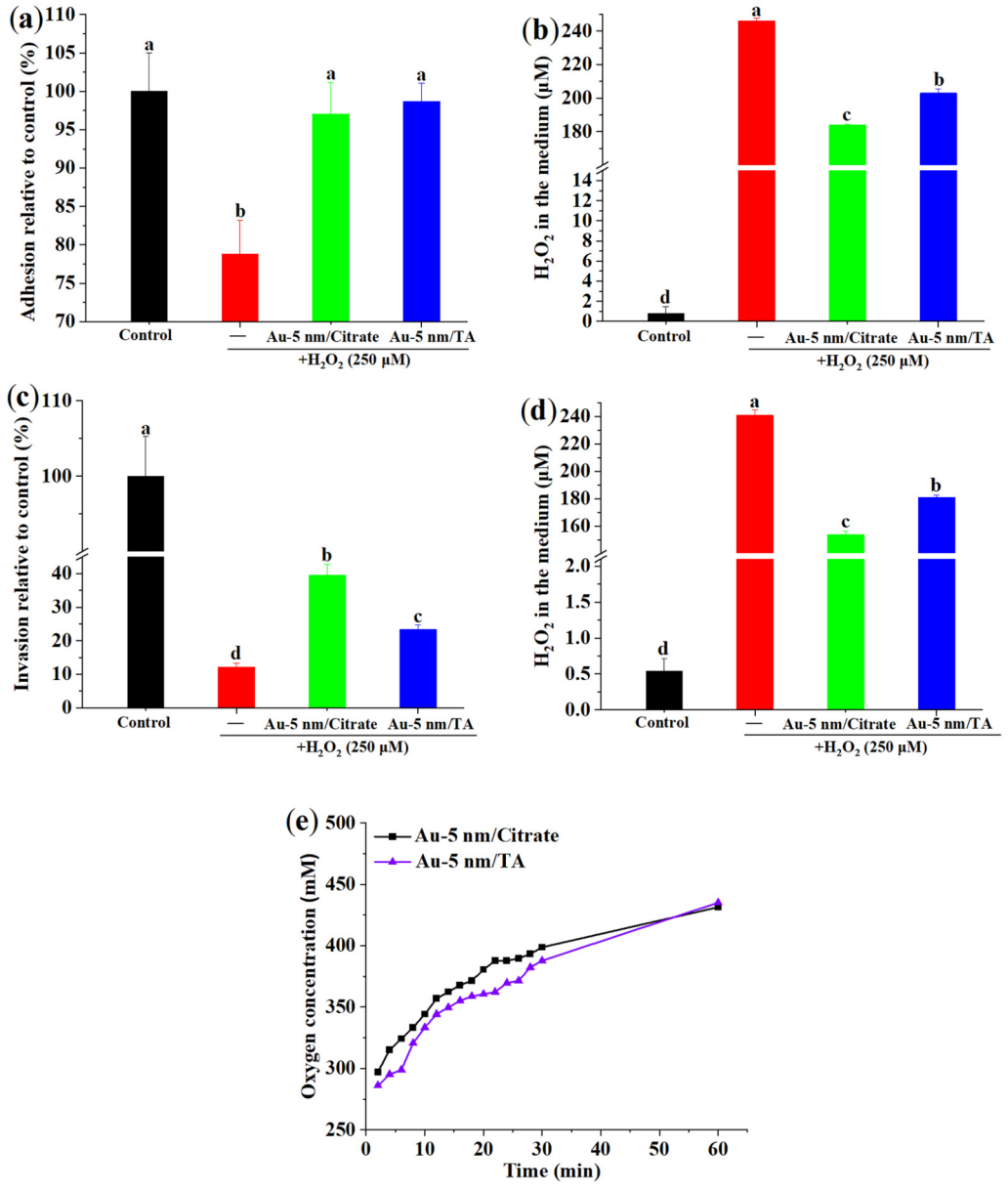

Figure 7 Effects of AuNPs on *S.* T (a) adhesion and (c) invasion against Caco-2 cell monolayers in the presence of H_2O_2, the residual H_2O_2 concentration in the co-culture medium after the (c) adhesion and (d) invasion assays, and (e) the catalase-mimetic activity of AuNPs determined by ESR oximetry. The comparison is made by using one-way ANOVA with LSD with different lower-case letters marking significant differences ($P < 0.05$).

Scientific and Technological Innovation Project in Shandong Province (No. 2022CXGC020414).

Declaration of competing interest

All the contributing authors report no conflict of interests in this work.

Author contribution statement

X. Y. G.: Data curation, validation, writing manuscript. M. K. B.: Data curation, validation, experimental design. Y. L.: Data curation. X. M. J.: experimental design. J.-J. Y.: Experimental design. H. H. W.: Project administration. S. Q. Z.: Project administration, funding acquisition, writing manuscript.

Informed consent

Not applicable.

Ethics statement

The animal experiments were carried ethically following the principles in the National Institutes of Health Guide for the Care and Use of Laboratory Animals and were approved by the Committee on the Ethics of Animal Experiments of Ocean University of China.

Use of AI statement

None.

References

[1] Xuan, L. H.; Ju, Z.; Skonieczna, M.; Zhou, P. K.; Huang, R. X. Nanoparticles-induced potential toxicity on human health: Applications, toxicity mechanisms, and evaluation models. *MedComm* **2023**, *4*, e327.

[2] Ma, Y.; Zhang, J. H.; Yu, N. R.; Shi, J. Q.; Zhang, Y.; Chen, Z. J.; Jia, G. Effect of nanomaterials on gut microbiota. *Toxics* **2023**, *11*, 384.

[3] Han, X. S.; Avelar, E.; Mathai, A.; Vollmer, D.; Lehman, R. A clinical study to evaluate the safety and efficacy of oral administration of microscopic dose gold nanoparticle (AuNP) on knee joint health and function in arthritis patients. *J. Funct. Morphol. Kinesiol.* **2022**, *7*, 52.

[4] Utembe, W.; Tlotleng, N.; Kamng'ona, A. A systematic review on the effects of nanomaterials on gut microbiota. *Curr. Res. Microb. Sci.* **2022**, *3*, 100118.

[5] Zhu, S. Q.; Jiang, X. M.; Boudreau, M. D.; Feng, G. X.; Miao, Y.; Dong, S. Y.; Wu, H. H.; Zeng, M. Y.; Yin, J. J. Orally administered gold nanoparticles protect against colitis by attenuating toll-like receptor 4- and reactive oxygen/nitrogen species-mediated inflammatory responses but could induce gut dysbiosis in mice. *J. Nanobiotechnol.* **2018**, *16*, 86.

[6] Madhogaria, B.; Bhowmik, P.; Kundu, A. Correlation between human gut microbiome and diseases. *Infect. Med.* **2022**, *1*, 180–191.

[7] Teklemariam, A. D.; Al-Hindi, R. R.; Albiheyri, R. S.; Alharbi, M. G.; Alghamdi, M. A.; Filimban, A. A. R.; Al Mutiri, A. S.; Al-Alyani, A. M.; Alseghayer, M. S.; Almaneea, A. M. et al. Human salmonellosis: A continuous global threat in the farm-to-fork food safety continuum. *Foods* **2023**, *12*, 1756.

[8] Safavieh, M.; Nahar, S.; Zourob, M.; Ahmed, M. U. Microfluidic biosensors for high throughput screening of pathogens in food. In *High Throughput Screening for Food Safety Assessment*. Bhunia, A. K.; Kim, M. S.; Taitt, C. R., Eds.; Elsevier: Amsterdam, 2015; pp 327–357.

[9] Stecher, B.; Robbiani, R.; Walker, A. W.; Westendorf, A. M.; Barthel, M.; Kremer, M.; Chaffron, S.; Macpherson, A. J.; Buer, J.; Parkhill, J. et al. *Salmonella enterica* serovar typhimurium exploits inflammation to compete with the intestinal microbiota. *PLoS Biol.* **2007**, *5*, 2177–2189.

[10] Di Marzo, N.; Chisci, E.; Giovannoni, R. The role of hydrogen peroxide in redox-dependent signaling: Homeostatic and pathological responses in mammalian cells. *Cells* **2018**, *7*, 156.

[11] Allaoui, A.; Botteaux, A.; Dumont, J. E.; Hoste, C.; De Deken, X. Dual oxidases and hydrogen peroxide in a complex dialogue between host mucosae and bacteria. *Trends Mol. Med.* **2009**, *15*, 571–579.

[12] Knaus, U. G.; Hertzberger, R.; Pircalabioru, G. G.; Yousefi, S. P. M.; Branco Dos Santos, F. Pathogen control at the intestinal mucosa-H_2O_2 to the rescue. *Gut Microbes* **2017**, *8*, 67–74.

[13] Vinayamohan, P.; Joseph, D.; Viju, L. S.; Baskaran, S. A.; Venkitanarayanan, K. Efficacy of probiotics in reducing pathogenic potential of infectious agents. *Fermentation* **2024**, *10*, 599.

[14] Zhu, S. Q.; Zeng, M. Y.; Guo, W.; Feng, G. X.; Wu, H. H. Catalase-mimetic gold nanoparticles inhibit the antagonistic action of *Lactobacillus gasseri* toward foodborne enteric pathogens in associative cultures. *J. Environ. Sci. Health, C Environ. Carcinog. Ecotoxicol. Rev.* **2019**, *37*, 55–66.

[15] Walker, G. T.; Gerner, R. R.; Nuccio, S. P.; Raffatellu, M. Murine models of *Salmonella* infection. *Curr. Protocol.* **2023**, *3*, e824.

[16] Barthel, M.; Hapfelmeier, S.; Quintanilla-Martínez, L.; Kremer, M.; Rohde, M.; Hogardt, M.; Pfeffer, K.; Rüssmann, H.; Hardt, W. D. Pretreatment of mice with streptomycin provides a *Salmonella enterica* serovar typhimurium colitis model that allows analysis of both pathogen and host. *Infect. Immun.* **2003**, *71*, 2839–2858.

[17] Zwietering, M. H.; Jongenburger, I.; Rombouts, F. M.; Van'T Riet, K. Modeling of the bacterial growth curve. *Appl. Environ. Microbiol.* **1990**, *56*, 1875–1881.

[18] Burkholder, K. M.; Bhunia, A. K. *Salmonella enterica* serovar Typhimurium adhesion and cytotoxicity during epithelial cell stress is reduced by *Lactobacillus rhamnosus* GG. *Gut Pathogens* **2009**, *1*, 14.

[19] Chandran, P.; Riviere, J. E.; Monteiro-Riviere, N. A. Surface chemistry of gold nanoparticles determines the biocorona composition impacting cellular uptake, toxicity and gene expression profiles in human endothelial cells. *Nanotoxicology* **2017**, *11*, 507–519.

[20] Aillon, K. L.; Xie, Y. M.; El-Gendy, N.; Berkland, C. J.; Forrest, M. L. Effects of nanomaterial physicochemical properties on *in vivo* toxicity. *Adv. Drug Delivery Rev.* **2009**, *61*, 457–466.

[21] Sharma, N.; Kurmi, B. D.; Singh, D.; Mehan, S.; Khanna, K.; Karwasra, R.; Kumar, S.; Chaudhary, A.; Jakhmola, V.; Sharma, A. et al. Nanoparticles toxicity: An overview of its mechanism and plausible mitigation strategies. *J. Drug Targeting* **2024**, *32*, 457–469.

[22] Wang, L. R.; Zhang, C. L.; Zhi, X.; Hou, W. X.; Li, T. L.; Pan, S. J.; Liu, B.; Song, J.; Pan, Y. X.; Ni, J. et al. Impact of short-term exposure of AuNCs on the gut microbiota of BALB/c mice. *J. Biomed. Nanotechnol.* **2019**, *15*, 779–789.

[23] Deng, Z.; Yang, C.; Xiang, T. W.; Dou, C.; Sun, D.; Dai, Q. J.; Ling, Z. G.; Xu, J. Z.; Luo, F.; Chen, Y. Q. Gold nanoparticles exhibit anti-osteoarthritic effects via modulating interaction of the "microbiota-gut-joint" axis. *J. Nanobiotechnol.* **2024**, *22*, 157.

[24] Li, J. J.; Cha, R. T.; Zhao, X. H.; Guo, H. B.; Luo, H. Z.; Wang, M. Z.; Zhou, F. S.; Jiang, X. Y. Gold nanoparticles cure bacterial infection with benefit to intestinal microflora. *ACS Nano* **2019**, *13*, 5002–5014.

[25] Saed, M.; Ayivi, R. D.; Wei, J. J.; Obare, S. O. Gold nanoparticles antibacterial activity: Does the surface matter. *Colloid Interface Sci. Commun.* **2024**, *62*, 100804.

[26] Pridmore, R. D.; Pittet, A. C.; Praplan, F.; Cavadini, C. Hydrogen peroxide production by *Lactobacillus johnsonii* NCC 533 and its role in anti-*Salmonella* activity. *FEMS Microbiol. Lett.* **2008**, *283*, 210–215.

[27] Atassi, F.; Servin, A. L. Individual and co-operative roles of lactic acid and hydrogen peroxide in the killing activity of enteric strain *Lactobacillus johnsonii* NCC933 and vaginal strain *Lactobacillus gasseri* KS120.1 against enteric, uropathogenic and vaginosis-associated pathogens. *FEMS Microbiol. Lett.* **2010**, *304*, 29–38.

[28] Mathur, R.; Oh, H.; Zhang, D. K.; Park, S. G.; Seo, J.; Koblansky, A.; Hayden, M. S.; Ghosh, S. A mouse model of *Salmonella typhi* infection. *Cell* **2012**, *151*, 590–602.

[29] Aili, M.; Zhou, K. B.; Zhan, J.; Zheng, H. P.; Luo, F. Anti-inflammatory role of gold nanoparticles in the prevention and treatment of Alzheimer's disease. *J. Mater. Chem. B* **2023**, *11*, 8605–8621.

[30] Botteaux, A.; Hoste, C.; Dumont, J. E.; Van Sande, J.; Allaoui, A. Potential role of Noxes in the protection of mucosae: H_2O_2 as abacterial repellent. *Microbes Infect.* **2009**, *11*, 537–544.

[31] Wang, S. G.; Lawson, R.; Ray, P. C.; Yu, H. T. Toxic effects of gold nanoparticles on *Salmonella* typhimurium bacteria. *Toxicol. Ind. Health* **2011**, *27*, 547–554.

[32] Buvelot, H.; Roth, M.; Jaquet, V.; Lozkhin, A.; Renzoni, A.; Bonetti, E. J.; Gaia, N.; Laumay, F.; Mollin, M.; Stasia, M. J. et al. Hydrogen peroxide affects growth of *S.* aureus through downregulation of genes involved in pyrimidine biosynthesis. *Front. Immunol.* **2021**, *12*, 673985.